

ANOMALOUS RESISTANCE OF PLASMA DURING TURBULENT HEATING

Yu. G. KALININ, A. S. KINGSEP, D. N. LIN, V. D. RYUTOV, and V. A. SKORYUPIN

Submitted July 10, 1969

Zh. Eksp. Teor. Fiz. 58, 68–75 (January, 1970)

Results are reported of measurements of the plasma resistance as a function of the initial experimental conditions during turbulent heating by a current. It is shown that the plasma resistance decreases approximately as $1/\sqrt{n}$ for densities between 10^{12} and 10^{14} cm^{-3} . The resistance is independent of the strength of the confining magnetic field when the latter varies between 5 and 21 kOe. The experimental results are used to calculate the ratio of the current velocity to the ion sound velocity. This ratio varies from 1.5 to 10 as the density is varied from 10^{14} to 5×10^{11} cm^{-3} . The resulting relations and the turbulent heating are explained in terms of the excitation of an ion acoustic instability in plasma by the current.

1. INTRODUCTION

THERE is a substantial number of papers in the literature^[1-5] reporting the results of studies of the anomalous resistance as a function of the initial plasma parameters such as the charged-particle density, ion mass, and the longitudinal electric field. In one of these papers^[4] it is proposed that the anomalous resistance is due to the excitation of the ion acoustic instability by the current, whereas elsewhere^[3,5] it is suggested that this resistance can be explained in terms of the excitation of the Buneman instability by the current.

In our previous experiments^[6,7] we gave most attention to the study of the effectiveness of turbulent heating. It was assumed that the anomalous resistance and plasma heating observed in these experiments were a consequence of the excitation of the ion acoustic instability by the longitudinal current in the plasma^[8]. This hypothesis is supported by experimental facts such as the substantial level (0.02nT–0.1nT) of ion acoustic oscillations as well as a number of other experimental data^[9-12].

The aim of the present work was to investigate the dependence of the anomalous resistance on the charged-particle density in plasma confined in a trap and on the magnetic field. We also report studies of the bremsstrahlung x rays from the anode of the direct discharge, and the dependence of the diamagnetic properties of the plasma on the duration of the current.

2. METHOD AND EXPERIMENTAL RESULTS

The experiments were carried out with the NPR-2 installation^[11]. Plasma parameters were chosen to lie in the following ranges: initial density n_0 between 5×10^{11} and 10^{14} cm^{-3} , and confining magnetic field H_0 between 5 and 21 kOe, which corresponded to ratios of the plasma frequency ω_{pe} to the electron cyclotron frequency ω_{He} between 0.16 and 10. The initial potential difference V_0 across the direct-discharge capacitor was 25 kV in all experiments, which meant that the mean electric field strength in the discharge gap was about 1 cgs esu. We measured the current through the discharge gap, the density, the diamagnetic properties of the plasma, and the x-rays due to the electrons striking the anode, all as functions of time.

The maximum plasma density in the trap was determined by microwave absorption methods. We used three generators with wavelengths of 0.4, 0.8, and 3.0 cm, which gave us the following density ranges: $n_0 < 1.1 \times 10^{12}$ cm^{-3} , 1.1×10^{12} $\text{cm}^{-3} < n_0 < 1.7 \times 10^{13}$ cm^{-3} , $1.7 \times 10^{13} < n_0 < 7 \times 10^{13}$ cm^{-3} and $n_0 > 7 \times 10^{13}$ cm^{-3} .

The current $I(t)$ flowing through the plasma was measured by a Rogowski loop with a bandwidth of about 10 MHz. The signal from this loop was applied to the plates of a fast oscillograph. The current circuit incorporated a capacitor of $C = 0.2$ μF , in which the energy was initially stored. The inductance L and resistance R of the circuit consisted of the resistance and inductance of the plasma column and the resistance and inductance of the leads. To determine the latter we used the following method. The plasma between the electrodes in the direct discharge was replaced by metal tubes of different diameters. The oscillation period was then used to determine the inductance of the leads, which turned out to be $L_0 = 400$ cm, and the damping of the oscillations was used to establish the resistance which was found to be $R_0 \approx 0.1$ Ω .

The plasma resistance $R_{pl}(t)$ can be determined from the energy balance equation

$$\frac{CV\dot{\phi}^2}{2} = \frac{CV^2(t)}{2} + \frac{(L_0 + L_{pl})I^2(t)}{2} \int_0^t [R_{pl}(\tau) + R_0]I^2(\tau)d\tau, \quad (1)$$

where L_{pl} is the inductance of the plasma column. Hence it follows that

$$R_{pl}(t) = \frac{V_0}{I} - \frac{1}{CI} \int_0^t I(\tau)d\tau - \frac{L_0 + L_{pl}}{I} \frac{\partial I}{\partial t} - \frac{1}{2} \frac{\partial L}{\partial t} - R_0. \quad (2)$$

To calculate R_{pl} we must know the current and the derivative and integral of the current. The last two quantities were determined graphically by analyzing the oscillograms. In addition, we must know the inductance L_{pl} of the plasma column itself and its derivative $\partial L_{pl}/\partial t$. These quantities can be found from measurements of the distribution of the azimuthal magnetic field H_ϕ over the cross section of the plasma column.

The azimuthal magnetic field of the current was measured by a system of seven single-turn probes distributed radially in the chamber. The diameter of each probe was 0.8 cm and the separation between them 1.3 cm. The signals were integrated by RC chains and

after amplification by a seven-channel broadband amplifier they were applied to the plates of the oscillographs. In this way the distribution of H_φ and hence the radial distribution of current density were determined at each instant of time. The total current through the plasma was measured at the same time with the Rogowski loop.

Figure 1 shows the radial current-density distribution in the chamber at the end of 0.12 (histogram a), 0.25 (histogram b), and 0.38 μ sec (histogram c) after the current was switched-on for densities in the range $1.7 \times 10^{13} \text{ cm}^{-3} < n_0 < 7 \times 10^{13} \text{ cm}^{-3}$ and $H_0 = 10^4$ Oe. It follows from the figure that in the time interval between 0.25 and 0.3 μ sec the current distribution remained constant although the total current increased. Most of the current (about 85%) was localized in a column 8 cm in diameter. The current density in this part of the chamber was not very dependent on the radial distance. At this time the inductance of the plasma column was 150 cm, while $I\partial L/\partial T \ll (L_0 + L_{pl})\partial I/\partial t$ and the corresponding term in Eq. (2) could be neglected.

For $t > 0.3 \mu$ sec the current distribution becomes very time-dependent. The rapid redistribution of the current density over the cross section means that accurate determination of $L(t)$ and $\partial L/\partial t$ and, consequently, $R_{pl}(t)$ becomes difficult. Anomalies in other plasma column characteristics appear at the same time (see below).

It is interesting to note the appearance of currents near the wall, which can be seen in Fig. 1. We may suppose that these currents are associated with the skin effect in the cold plasma near the wall, in the magnetic field of the current flowing between the electrodes.

The x-rays were detected through an aperture at the center of the anode which was 0.2 cm in diameter and was covered by an 18- μ beryllium foil. The x-ray detector (stilbene crystal + FEU-13 photomultiplier) was placed 150 cm from the foil. The space between the foil and the crystal was pumped down to 0.01 Torr. We estimated that 1.2-keV x-rays were attenuated by a factor of e in this system.

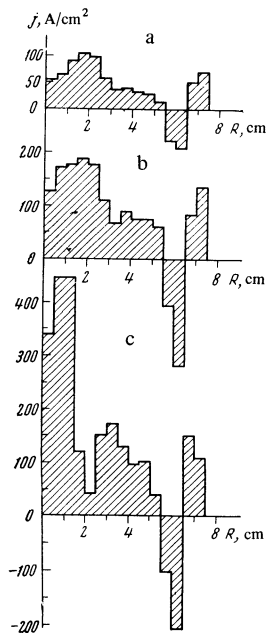


FIG. 1. Radial distribution of current density in the plasma column: a - $t = 0.12$, b - $t = 0.25$, c - $t = 0.38 \mu$ sec.

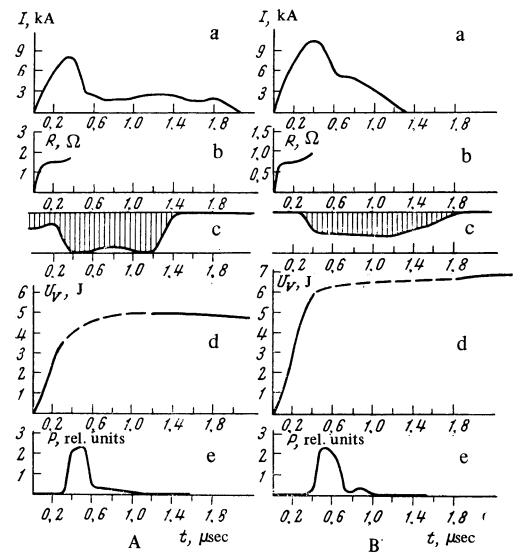


FIG. 2. Plasma parameters as functions of time: A - initial density in the range $1.1 \times 10^{12} \text{ cm}^{-3} < n_0 < 10^{13} \text{ cm}^{-3}$, B - initial density in the range $1.7 \times 10^{13} \text{ cm}^{-3} < n_0 < 7 \times 10^{13} \text{ cm}^{-3}$. Oscillogram a - current through plasma, b - resistance of plasma column, c - transmission curve for 0.8 cm radiation, d - plasma energy content, e - x-ray emission from the anode.

The energy content of the plasma was estimated as follows. The magnetic flux displaced by the plasma was measured by a single-turn probe around the plasma and the return current leads. The confining magnetic field varied with a period of 3 msec and, therefore, use was made of a ten-turn compensating probe whose total area was equal to the area of the main probe. The compensating probe turns were placed inside the solenoid but did not cover the plasma and were connected in opposition to the main probe. This enabled us to reduce the parasitic signal from the confining field by a factor of about 5000.

If the magnetic flux displaced by the hot plasma is $\Delta\Phi$, the flux outside the plasma in the solenoid increases by the same amount. The total flux measured by both probes connected in opposition is $\Delta\Phi S/(S - S_{pl})$, where $S = 500 \text{ cm}^2$ and S_{pl} are the cross-section areas of the solenoid and the plasma, respectively. Since $S_{pl} \ll S$, it may be assumed that the system measures the flux displaced by the plasma. The total energy content of the plasma column is calculated from the formula

$$U_v \approx 0.8 V_p H_0 l \tau + 5 \cdot 10^{-10} I^2, \quad (3)$$

where V_p is the probe signal in volts, H_0 is the confining magnetic field in Oe, l is the distance between the magnetic mirrors in cm, $\tau = 10^{-4}$ sec is the time constant of the integrating network, and I is the current through the plasma in amperes.

Figure 2 shows oscillograms of the current (a), x-ray intensity (e), energy content (d), total resistance of the plasma column (b), and the transmission of 0.8 cm radiation (c). The resistance and energy content were calculated from Eqs. (2) and (3), respectively. In the experiments shown in Fig. 2a the initial concentration was in the range $1.1 \times 10^{12} \text{ cm}^{-3} < n_0 < 7 \times 10^{13} \text{ cm}^{-3}$, whereas in Fig. 2b it was in the range $1.7 \times 10^{13} \text{ cm}^{-3} < n_0 < 7 \times 10^{13} \text{ cm}^{-3}$. In both experiments $H_0 = 10 \text{ kOe}$.

A similar analysis of the plasma heating process was also carried out for initial concentrations $n_0 < 1.1 \times 10^{12} \text{ cm}^{-3}$ and $n_0 > 7 \times 10^{13} \text{ cm}^{-3}$ for three values of the confining magnetic field (5, 10, and 21 kOe). It was established in all three cases that the discharge occurred in two stages.

During the first stage there is fast heating of the plasma, and the plasma column is relatively stable. The heating efficiency is constant and amounts to about 30%. The energy content of the plasma during this stage increases to practically its final value which is determined by the displaced flux when the current passes through zero for the first time. A rapid change in the column configuration (histogram c in Fig. 1) begins during the second stage and is followed by a rapid reduction in the maximum density in the column (curves c in Fig. 2). At the same time, there are strong anomalies on the diamagnetic signal oscillogram. It is clear from Fig. 2e that there are no x rays during the initial stage of the process. Insufficient sensitivity of the detection system prevented us from carrying out accurate quantitative estimates but, in any case, it can be concluded that the mean energy of electrons transporting the current during this time was less than 3 keV. Hard x rays appeared during the second stage. The maximum energy of electrons giving rise to this radiation can be estimated as 15–20 keV. The estimated intensities indicate that these electrons are responsible for 0.1 of the current.

The duration of the first stage of the process and the energy content of the plasma increase with increasing initial density. The time of quiescent heating varies from 0.15–0.2 to 0.4–0.45 μsec , and the energy content U_V from 3 to 7 J when the initial plasma density increases from about 10^{12} to about 10^{14} cm^{-3} .

To determine the plasma energy content as a function of the time for which the current flows, we performed an additional experiment. Some time after the current was switched on, the direct discharge capacitor was shorted by a special discharger, and the influx of energy into the plasma was terminated. The time between the instant at which the current was switched on and the shorting of the capacitor could be varied. Figure 3 shows the integrated energy content of the plasma as a function of the time of heating (curve b). All the points were obtained with the following initial parameters: $H_0 = 10 \text{ kOe}$, $1.7 \times 10^{13} \text{ cm}^{-3} < n_0 < 7 \times 10^{13} \text{ cm}^{-3}$. Figure 3 shows the current (curve a) as a function of time with the shorting device open. The integrated energy content was determined from the total displaced flux 0.5 μsec after shorting, when the current through the plasma was zero. If we assume that energy losses during this time are negligible, the resulting curve (Fig. 3b) represents the energy content as a function of time with the shorting device open.

Comparison of the energy-content curves in Figs. 2 and 3 shows that, during the first 0.3 μsec following the instant at which the current is switched off, the curves obtained by different methods are virtually the same. Next, according to Fig. 3, plasma heating has practically terminated although at time $t = 0.3 \mu\text{sec}$ the capacitor still holds more than 60% of the energy.

Figure 3 also shows the integrated energy flux across the magnetic field at the center of the trap as a function

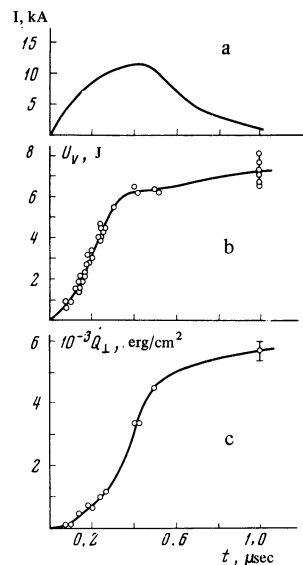


FIG. 3

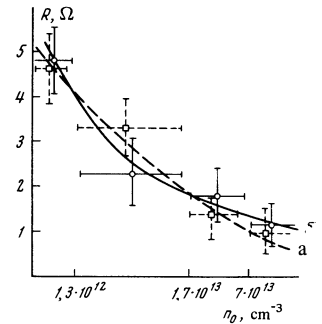


FIG. 4

FIG. 3. Plasma parameters as functions of time of current flow: a – current through plasma with shorting gap switched off, b – energy content as a function of time of current flow, c – energy flux across the magnetic field as a function of the time of current flow.

FIG. 4. Plasma resistance as a function of initial density: a – confining field $H_0 = 5 \text{ kOe}$, b – confining field $H_0 = 21 \text{ kOe}$.

of heating time (curve c). The energy flux was measured with a bismuth bolometer^[13] mounted on a tube at a distance of 8 cm from the chamber axis. The wall energy losses increase rapidly after the instant corresponding to the end of the heating process, and the second stage begins. However, the wall losses are much less (roughly by a factor of ten) than the total energy remaining in the capacitor at a time when the second stage begins. It is shown in^[11] that most of this energy is dissipated in the anode.

The anomalous plasma resistance was calculated from Eq. (2), but this calculation is possible only for the first stage. It is clear from Fig. 2b that after the current is switched on the resistance increases rapidly in a time $t_0 \leq 0.05 \mu\text{sec}$ and thereafter varies slowly throughout the initial stage. We note that the characteristic growth rate of the ion acoustic instability is

$$\gamma \sim \omega_{pi} \sqrt{m/M}, \quad (4)$$

where m is the electron mass, M is the hydrogen-ion mass, and ω_{pi} is the ion plasma frequency. According to Eq. (4), the resistance growth time is 0.01 μsec .

The plasma resistance decreases with increasing density. Figure 4 (curve a) shows the plasma resistance as a function of initial density for $H_0 = 5 \text{ kOe}$ and 21 keV (curve b). In all the experiments the resistance was measured at 0.1 μsec after the current was switched on. An average over 10–12 experiments correspond to each point. As can be seen, curves a and b in Fig. 4 coincided to within experimental error.

An investigation was also made of the ratio of the streaming velocity u to the ion sound velocity c_s as a function of the initial parameters. This ratio was calculated from

$$u/c_s = I\sqrt{M}/S_{p1}ne\sqrt{T_e}, \quad (5)$$

where e is the electron charge and T_e is the electron

temperature in cgs esu. The values of all the quantities which are necessary for the calculation of u/c_s were taken at $t = 0.1 \mu\text{sec}$. The results of the calculations are shown in Fig. 5. The ratio u/c_s does not exceed 10 and falls monotonically, roughly as $1/\sqrt{n}$, with increasing initial density. This ratio is independent of the magnetic field H_0 within the chosen range of magnetic fields.

3. DISCUSSION OF RESULTS

The main results of measurements shown in Figs. 1–5 can be explained as follows. During the first stage of the process there are no large-scale hydrodynamic instabilities in the plasma, and the density of the plasma column and the current distribution over its cross section remain constant. The ratio of the streaming velocity to the ion sound velocity measured at this stage approaches unity in the broad density range 10^{12} – 10^{14} cm^{-3} . During the initial stage of the current there are no beam electrons with energies $\geq 3 \text{ keV}$ which would be capable of transporting the entire plasma current. This leads us to the conclusion that the turbulent plasma heating observed during the first stage is not associated with the beam. Consequently, the heating can only be associated with the development of current instability. When $u/c_s < 40$, only the ion acoustic instability is possible. The growth time of the anomalous resistance is equal, to within experimental error, to the characteristic time for the development of the ion acoustic instability. It is important to note that the magnitude of the anomalous resistance (Fig. 4) is independent of the strength of the confining magnetic field. Finally, measurements of the noise spectrum at frequencies approaching the ion plasma frequency, which were reported earlier in^[12], indicate the presence of high-intensity ion acoustic oscillations in the plasma.

All this supports the hypothesis that the observed heating is connected with the development of ion acoustic instability in the plasma. We note particularly the high efficiency ($\sim 30\%$) observed during the initial stage of the heating process and the relatively low energy flux to the chamber walls (curve c, Fig. 3).

Next, large-scale hydrodynamic instability grows in plasma after a certain instant of time. This is probably the current convective instability which develops in plasma with anomalous resistance at a very high growth rate.¹⁾ This is indicated, firstly, by the rapid redistribution of current over the cross section of the chamber (Fig. 1), secondly, by the rapid fall of the maximum density measured by the microwave absorption method (Fig. 2) and, thirdly, by the large-scale fluctuations in the magnetic field due to the current, noted in^[12]. The

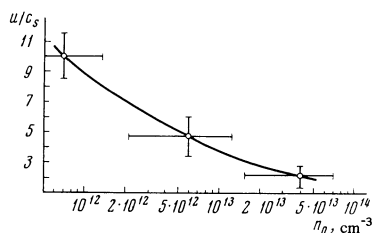


FIG. 5. The ratio u/c_s as a function of initial plasma density.

anomalies on the diamagnetic signal curve can be explained by the fact that, as a result of anomalous diffusion due to the development of large-scale instability, the plasma is found to expand and comes into contact with the chamber walls. When this is so, the value of U_V calculated from Eq. (3) should be low.

Additional measurements (Fig. 3) show that there is no substantial heating of the plasma during the second stage, nor is there any reduction in the energy content of the plasma column followed by substantial heating. It follows that the process of accumulation of energy in the plasma may be regarded as complete at the time of transition from quiescent heating to the development of large-scale instability. The equilibrium between the absorption of energy and losses which are expended largely at the anode of the discharge is established next.

In conclusion, the authors wish to thank E. K. Zavoiskii and L. I. Rudakov for their constant interest and advice in this research.

¹S. D. Fanchenko, B. A. Demidov, N. I. Elagin, and D. D. Ryutov, Zh. Eksp. Teor. Fiz. 46, 497 (1964) [Sov. Phys.-JETP 19, 337 (1964)].

²P. Ya. Burchenko, B. T. Vasilenko, E. D. Volkov, R. M. Nikolaev, V. A. Potapenko, and V. T. Tolok, ZhETF Pis. Red. 3, 243 (1966) [JETP Lett. 3, 156 (1966)].

³V. A. Ruprunenko, E. A. Sukhomlin, and N. I. Reva, Atomnaya Énergiya 17, 83 (1964).

⁴B. A. Demidov, N. I. Elagin and S. D. Fanchenko, Dokl. Akad. Nauk SSSR 174, 327 (1967) [Sov. Phys.-Doklady 12, 467 (1967)].

⁵J. H. Adlam, D. E. T. F. Ashby, R. J. Bickerton, J. N. Burcham, M. Friedman, S. M. Hamberger, E. S. Hotston, D. J. Lees, A. Malein, R. Reynolds, and P. A. Shatford, White. Third conference on plasma physics and controlled nuclear fusion research, CN-24/D-8, Novosibirsk, 1968.

⁶M. V. Babykin, P. P. Gavrin, E. K. Zavoiskii, L. I. Rudakov and V. A. Skoryupin, Zh. Eksp. Teor. Fiz. 47, 1597 (1964) [Sov. Phys.-JETP 20, 1073 (1965)]. Second International Conference on Plasma Physics, Culham, England, 1965, paper CN-21/154.

⁷M. V. Babykin, P. P. Gavrin, E. K. Zavoiskii, S. L. Nedoseev, L. I. Rudakov and V. A. Skoryupin, Zh. Eksp. Teor. Fiz. 52, 643 (1967) [Sov. Phys.-JETP 25, 421 (1967)].

⁸L. I. Rudakov and L. V. Korablev, Zh. Eksp. Teor. Fiz. 50, 220 (1966) [Sov. Phys.-JETP 23, 145 (1966)].

⁹D. N. Lin and V. A. Skoryupin, Zh. Eksp. Teor. Fiz. 53, 463 (1967) [Sov. Phys.-JETP 26, 305 (1968)].

¹⁰Yu. G. Kalinin, D. N. Lin, V. D. Ryutov, and V. A. Skoryupin, Zh. Eksp. Teor. Fiz. 55, 115 (1968) [Sov. Phys.-JETP 18, 61 (1969)].

¹¹Yu. G. Kalinin, D. N. Lin, V. D. Ryutov, and V. A. Skoryupin, Zh. Eksp. Teor. Fiz. 56, 462 (1969) [Sov. Phys.-JETP 29, 000 (1969)].

¹²Yu. G. Kalinin, D. N. Lin, L. I. Rudakov, V. D. Ryutov, and V. A. Skoryupin, Dokl. Akad. Nauk SSSR 89, No. 2 (1969) [Sov. Phys.-Doklady 14, No. 11 (1970)].

¹³L. L. Gorelik and V. V. Sinitsyn, Zh. Tekh. Fiz. 32, 1406 (1962) [Sov. Phys.-Tech. Phys. 7, 1036 (1963)].

¹⁾This was first suggested by L. I. Rudakov.